Dalton Transactions

Cite this: *Dalton Trans.*, 2011, **40**, 7412

www.rsc.org/dalton

PAPER

Synthesis, structural characterization, photophysical properties and theoretical analysis of gold(I) thiolate-phosphine complexes†

Igor O. Koshevoy,*[a] Ekaterina S. Smirnova,[a,b] Matti Haukka,[a] Antonio Laguna,*[b] Jessica Camara Chueca,[b] Tapani A. Pakkanen,[a] Sergey P. Tunik,*[c] Isaura Ospino[b] and Olga Crespo[b]

Received 15th March 2011, Accepted 5th May 2011
DOI: 10.1039/c1dt10437c

A series of luminescent dinuclear neutral complexes of stoichiometry $[(AuSPh)_2(PPh_2\text{-}(C_6H_4)_n\text{-}PPh_2)]$ (n = 1, 2, 3) as well as their tetranuclear cationic derivatives $[(Au_2SPh)_2(PPh_2\text{-}(C_6H_4)_n\text{-}PPh_2)_2](PF_6)_2$ are reported. Their crystal structures have been elucidated by X-ray studies. These studies indicate that, for the dinuclear species, only when n = 1 the molecules exhibit intermolecular aurophilic interactions. None of the tetranuclear species crystallizes in their molecular form, due to the formation of aggregates through Au···Au interactions. The origin of the luminescence has been analyzed by computational studies indicating that the presence or absence of aurophilic interactions does not affect the luminescent behavior and that intraligand charge transfer processes which involve the thiolate and the diphosphine are responsible for the emissions. The result is in contrast with the thiolate–gold charge transfer processes which dominate the photophysics of gold-thiolate compounds and reveals the influence of the phenylene spacers in the emissive behavior of these compounds.

Introduction

The chemistry of gold(I) thiolate complexes has been extensively studied for decades. These continuing investigations have been stimulated by the general academic interest to this structurally versatile class of compounds,[1–10] demonstrating rich photophysical properties over a wide range of the visible spectrum.[9,11–20] Accessible modification of the organic functionalities of S-containing ligands and effectiveness of formation of gold(I) thiolate complexes allowed for the preparation of certain materials and structures on their basis,[7,19,21] as well as successful applications in the areas of medicine[22] and chemosensing.[10,23,24]

The structural variations of the polynuclear gold(I) thiolates arise, on the one hand, from the stereochemical diversity and bridging coordination of S-atom of the thiols, including the di- and tri-dentate ones.[1,5–7,14,15,25,26] On the other hand, employment of the multidentate ancillary ligands like phosphines gives additional possibilities for the construction of polymetallic complexes and clusters.[1,4,7,9,26–28] Additionally, Au···Au interactions, which often govern formation of the fascinating supramolecular structures, were found for many gold(I)-sulfur compounds both in the solid state and solution.[8,18,29,30]

According to the literature data, the photophysical characteristics of the gold(I) thiolates containing phosphine ligands are usually determined mainly by the ligand-to-metal (S"Au) charge transfer, the variation of the emission band is associated with the electron-withdrawing groups on the thiolate ligand and no correlation exists between the magnitude of the Au···Au distance and the observed emission energy.[9,11,20,31] Besides, it was noted that despite most aromatic phosphine ligands being emissive species, their intra-ligand luminescence does not appear, or appears only as a trace in the high-energy side, compared with the main emission originated from the S"Au charge transfer.[9]

Recently, we have been using tertiary diphosphines with oligophenylene spacers, $PPh_2\text{-}(C_6H_4)_n\text{-}PPh_2$ (n = 1, 2, 3),[32,33] in coordination chemistry of gold(I) alkynyl complexes. In order to extend our work we intended to investigate the related thiolate-diphosphine compounds—their structural arrangement and photophysical behavior in the solid state and solution. Herein we report synthesis, spectral and structural characterization, and the photoluminescent studies of the novel digold complexes $[(AuSPh)_2(PPh_2\text{-}(C_6H_4)_n\text{-}PPh_2)]$ and their tetranuclear cationic derivatives $[(Au_2SPh)_2(PPh_2\text{-}(C_6H_4)_n\text{-}PPh_2)_2](PF_6)_2$ (n = 1, 2, 3). The latter compounds were found to form supramolecular aggregate (n = 1) and polymeric structures (n = 2, 3) in the solid state. The emissive characteristics of these compounds unexpectedly were found to be mainly determined by metal perturbed intra-ligand (IL) electronic transitions in the bridging phosphine ligands that

[a]*University of Eastern Finland, Joensuu, 80101, Finland. E-mail: igor.koshevoy@uef.fi; Fax: +358 13 2513390; Tel: +358 13 2513325*
[b]*St.-Petersburg State University, Department of Chemistry, Universitetskii pr. 26, 198504, St.-Petersburg, Russia. E-mail: stunik@inbox.ru; Fax: +7 812 4283969; Tel: +7 812 4284028*
[c]*Universidad de Zaragoza-CSIC, Instituto de Ciencia de Materiales de Aragon, Departamento de Quimica Inorganica, E-50009, Zaragoza, Spain. E-mail: alaguna@unizar.es; Fax: + 34 976 761187; Tel: + 34 976 761185*

† Electronic supplementary information (ESI) available: X-ray crystallographic data in CIF for **1–6**, ^1H-^1H COSY spectra of **1–6**, ESI-mass spectra of **4–6**, the geometry of the modeled complex **4**. CCDC reference numbers 817752-817757. For ESI and crystallographic data in CIF or other electronic format see DOI: 10.1039/c1dt10437c

is in contrast with interpretation of the data obtained earlier for other gold(I) thiolate-phosphine complexes.

Experimental

General comments

[AuCl(tht)],[34] $(AuSPh)_n$,[35] $PPh_2(C_6H_4)_nPPh_2$ (n = 1, 2, 3),[33,36] $[Au_2(PPh_2(C_6H_4)_nPPh_2)_2](PF_6)_2$ (n = 1, 2, 3)[32,37] were synthesized according to published procedures. Other reagents and solvents were used as received. Solution ^1H and ^{31}P NMR spectra were recorded using Bruker Avance 400 and Bruker DPX 300 spectrometers. The chemical shifts (δ, ppm) were referenced to residual solvent resonances and external 85% H_3PO_4 in the ^1H and ^{31}P spectra, respectively. The 2D COSY spectra were run using standard Bruker pulse sequence. Mass spectra were determined on a Bruker APEX-Qe ESI FT-ICR instrument, in the ESI^+ mode, solvent CH_2Cl_2. Microanalyses were carried out in the analytical laboratory of St.-Petersburg State University. UV-Vis spectra were recorded on a Shimadzu UV 3600 spectrophotometer. DRUV spectra were recorded using an EVOLUTION 600 spectrophotometer equipped with a Praying Mantis diffuse reflectance accessory. Solid state samples were mixed with silica. The intensities were recorded in Kubelka-Munk units. Steady-state photoluminescence spectra were recorded with a Jobin-Yvon Horiba Fluorolog FL-3-11 spectrometer using band pathways of 3 nm for both excitation and emission. The lifetimes were measured using a Fluoromax phosphorimeter accessory containing a UV xenon flash tube. The lifetime data were fit using the Jobin-Yvon software package[38] and the Origin 5.0 program.[39]

[(AuSPh)$_2$(1,4-PPh$_2$C$_6$H$_4$PPh$_2$)] (1)

$(AuSPh)_n$ (137 mg, 0.448 mmol) was suspended in CH_2Cl_2 (15 cm^3) and slight excess of 1,4-$PPh_2C_6H_4PPh_2$ (108 mg, 0.242 mmol) was added. The reaction mixture was stirred for 1.5 h in the absence of light to give nearly transparent colorless solution. It was passed through a layer of silica (2 cm) and evaporated. Recrystallization from CH_2Cl_2/benzene/heptane mixture at +5 °C gave crystalline pale-yellowish solid, which was collected, washed with pentane and vacuum dried. Yield: 210 mg, 89%. $^{31}P\{^1H\}$ NMR ($CDCl_3$; δ): 38.1 (s). ^1H NMR ($CDCl_3$; δ): **Ph-thiolate** ligand: 7.62 (d, *ortho*-H, J = 7.7 Hz, 4H), 7.01 (t, *para*-H, J = 7.3 Hz, 2H), 7.12 (m, *meta*-H, J = 7.3, 7.7 Hz, 4H); **diphosphine**: 7.60–7.50 (m, 24H). Anal. Calc. for $C_{42}H_{34}Au_2P_2S_2$: C, 47.65; H, 3.24; S 6.06. Found: C, 47.75; H, 3.25; S 6.42.

[(AuSPh)$_2$(4,4′-PPh$_2$(C$_6$H$_4$)$_2$PPh$_2$)] (2)

Prepared analogously to **1** using $PPh_2(C_6H_4)_2PPh_2$ instead of $PPh_2C_6H_4PPh_2$. Yield: 95%. $^{31}P\{^1H\}$ NMR ($CDCl_3$; δ): 37.9 (s). ^1H NMR ($CDCl_3$; δ): **Ph-thiolate** ligand: 7.64 (d, *ortho*-H, J = 7.8 Hz, 4H), 7.01 (t, *para*-H, J = 7.3 Hz, 2H), 7.12 (m, *meta*-H, J = 7.3, 7.8 Hz, 4H); **diphosphine**: 7.71–7.66; 7.60–7.49 (m, 28H). Anal. Calc. for $C_{48}H_{38}Au_2P_2S_2$: C, 50.80; H, 3.38; S 5.65. Found: C, 50.74; H, 3.39; S 5.84.

[(AuSPh)$_2$(4,4′′-PPh$_2$(C$_6$H$_4$)$_3$PPh$_2$)] (3)

Prepared analogously to **1** using $PPh_2(C_6H_4)_3PPh_2$ instead of $PPh_2C_6H_4PPh_2$. Yield: 94%. $^{31}P\{^1H\}$ NMR ($CDCl_3$; δ): 37.8 (s). ^1H NMR ($CDCl_3$; δ): **Ph-thiolate** ligand: 7.65 (d, *ortho*-H, J = 7.8 Hz, 4H), 7.01 (t, *para*-H, J = 7.3 Hz, 2H), 7.13 (m, *meta*-H, J = 7.3, 7.8 Hz, 4H); **diphosphine**: 7.76–7.68; 7.62–7.49 (m, 32H). Anal. Calc. for $C_{54}H_{42}Au_2P_2S_2$: C, 53.56; H, 3.50; S 5.30. Found: C, 53.69; H, 3.41; S 5.58.

[(Au$_2$SPh)$_2$(1,4-PPh$_2$C$_6$H$_4$PPh$_2$)$_2$](PF$_6$)$_2$ (4)

The following reactions were carried out under nitrogen atmosphere.

Method A. $(AuSPh)_n$ (28 mg, 0.092 mmol) was suspended in CH_2Cl_2 (10 cm^3) and $[Au_2(PPh_2C_6H_4PPh_2)_2](PF_6)_2$ (71 mg, 0.045 mmol) was added. The reaction mixture was stirred overnight in the absence of light to give nearly transparent pale-yellowish solution. It was filtered and evaporated. Repetitious recrystallization from CH_2Cl_2/acetone/heptane mixture at room temperature gave colorless crystals of **4**, which were collected, washed with diethyl ether and vacuum dried. Yield: 65 mg, 66%.

Method B. Au(tht)Cl (32 mg, 0.1 mmol) was dissolved in CH_2Cl_2 (10 cm^3) and $PPh_2C_6H_4PPh_2$ (22.5 mg, 0.05 mmol) was added. The colorless transparent reaction mixture was stirred for 10 min and a solution of $AgPF_6$ (25.5 mg, 0.1 mmol) was added causing immediate precipitation of AgCl. The suspension was stirred for an additional 30 min, filtered and added to a solution of **1** (53 mg, 0.05 mmol) in CH_2Cl_2 (10 cm^3). The pale-yellowish reaction mixture was stirred for 3 h in the absence of light and then further treated as in method A. Yield: 76 mg, 70%. ES MS (m/z): $[(Au_2SPh)_2(PPh_2C_6H_4PPh_2)_2]^{2+}$ 949.1 (calcd 949). $^{31}P\{^1H\}$ NMR (CD_2Cl_2; δ): 36.0 (s), -143.0 (sept, 2P, PF_6). ^1H NMR (CD_2Cl_2; δ): Ph-thiolate ligand: 7.58 (4H, m, *ortho* protons), 7.23–7.31 (6H, AB system of *meta* and *para* protons); diphosphine: 7.26 (8H, protons of phenylene spacer, $A_2\times_2$ system, J(H-H) *ca.* 7 Hz, J(*P*-H) *ca.* 15 Hz), 7.60 (8H, t, *para*-H, J(H-H) *ca.* 7 Hz), 7.42 (16 H, m, *meta*-H, J(H-H) *ca.* 7 Hz), 7.48 (16H, m, *ortho*-H, J(H-H) *ca.* 7 Hz, J(*P*-H) *ca.* 13 Hz). Anal. Calc. for $C_{72}H_{58}Au_4F_{12}P_6S_2$: C, 39.50; H, 2.67; S 2.93. Found: C, 39.44; H, 2.59; S 2.77.

[(Au$_2$SPh)$_2$(4,4′-PPh$_2$(C$_6$H$_4$)$_2$PPh$_2$)$_2$](PF$_6$)$_2$ (5)

Prepared analogously to **4** (*method A*) using $[Au_2(PPh_2(C_6H_4)_2PPh_2)_2](PF_6)_2$ instead of $[Au_2(PPh_2C_6H_4PPh_2)_2](PF_6)_2$. Yield: 71% (method B 75%). ES MS (m/z): $[(Au_2SPh)_2(PPh_2(C_6H_4)_2PPh_2)_2]^{2+}$ 1025.1 (calcd 1025). $^{31}P\{^1H\}$ NMR (CD_2Cl_2; δ): 35.8 (s), -143.0 (sept, 2P, PF_6). ^1H NMR (CD_2Cl_2; δ): ABC system of **Ph-thiolate** ligand with the signal centered at: *meta*-H 7.30 (4H), *para*-H 7.41 (2H), *ortho*-H 7.43 (4H); **diphosphine**: 7.73 and 7.42 (m, -$P(C_6H_4)_2$P- 16H), 7.64 and 7.47–7.56 (m, PPh_2, 40H). Anal. Calc. for $C_{84}H_{66}Au_4F_{12}P_6S_2$: C, 43.09; H, 2.84; S 2.74. Found: C, 43.03; H, 3.02; S 2.55.

[(Au$_2$SPh)$_2$(4,4′′-PPh$_2$(C$_6$H$_4$)$_3$PPh$_2$)$_2$](PF$_6$)$_2$ (6)

Prepared analogously to **4** (*method A*) using $[Au_2(PPh_2(C_6H_4)_3PPh_2)_2](PF_6)_2$ instead of $[Au_2(PPh_2C_6H_4PPh_2)_2](PF_6)_2$. Yield: 84% (method B 91%). ES MS (m/z): $[(Au_2SPh)_2(PPh_2(C_6H_4)_3PPh_2)_2]^{2+}$ 1101.1 (calcd 1101). $^{31}P\{^1H\}$ NMR (CD_2Cl_2; δ): 35.5 (s), -143.0

(sept, 2P, PF_6). ^{1}H NMR (CD_2Cl_2; δ): **Ph-thiolate** ligand: 7.73 (4H, dd, *ortho* protons, J(H-H) *ca.* 8 and 1.4 Hz), 7.34–7.42 (6H, AB system of *meta* and *para* protons); **diphosphine**: 7.39 (8H, s, protons of central phenylene spacer), 7.62 (8H, $A_2\times_2$ m, *ortho*-protons of P-$C_6\underline{H}_4$ spacers, J(H-H) *ca.* 7 Hz, J(*P*-H) *ca.* 14 Hz), 7.48 (8H, d, *meta*-H of P-$C_6\underline{H}_4$ spacers, J(H-H) *ca.* 7 Hz), 7.44–7.56 (40 H, unresolved m, $PC_6\underline{H}_5$). Anal. Calc. for $C_{96}H_{74}Au_4F_{12}P_6S_2$: C, 46.24; H, 2.99; S2.57. Found: C, 46.32; H, 3.05; S 2.75.

X-Ray diffraction studies

The crystals of **1–6** were immersed in cryo-oil, mounted in a Nylon loop, and measured at a temperature of 100 K. The X-ray diffraction data were collected on a Nonius KappaCCD diffractometer using Mo-Kα radiation (λ = 0.710 73 Å). The *Denzo-Scalepack*[40] or *EvalCCD*[41] program packages were used for cell refinements and data reductions. The structures were solved by direct methods using the *SHELXS-97*,[42] *SIR97*,[43] or *SUPERFLIP*[44] programs with the *WinGX*[45] graphical user interface. A semi-empirical absorption correction (*SADABS*)[46] was applied to all data. Structural refinements were carried out using *SHELXL-97*.[42] The anisotropic displacement parameters of the adjacent carbon atoms in the phenyl rings were restrained to be similar. In **1** the geometry of CH_2Cl_2 solvent molecule was restrained by fixing C–Cl and Cl–Cl distances. The CH_2Cl_2 carbon (C45) was further restrained so that its U_{ij} components approximate to isotropic behavior. The crystal of **2** was found to be twinned *via* a 180° rotation about the direct axis (1,0,0). The two components were determined using the *ROTAX*[47] program and the BASF value was refined to 0.29. The asymmetric unit of **2** contains two benzenes, of which one is disordered over two sites with occupancies 0.61 and 0.39. A rigid bond restraint was applied to all carbon atoms of the disordered benzene molecules. The anisotropic displacement parameters in the direction of the bond were restrained to be equal within an s.u. of 0.01. Furthermore, carbon atoms C55A, C55B, and C42 were restrained so that their U_{ij} components approximate to isotropic behavior. Due to the poor data quality the structure of **2** is used solely as supporting material. In **4** the fluorine atoms of the PF_6^- anions were disordered over two sites with occupancy ratio 0.65/0.35. The fluorine atoms were refined with equal anisotropic displacement parameters. One of the acetone solvent molecules was also disordered over two sites with occupancies 0.53/0.47. Furthermore, one of the phenyl rings was disordered over two sites. The carbon atoms of the disordered rings were constrained with fixed C–C bond lengths and C–C–C angles (1.39 Å and 120° respectively). The occupancies were refined to 0.52/0.48. In **5** the CH_2Cl_2 solvent molecule was disordered over two sites with equal occupancies. Furthermore, the chlorine atoms in the second part of the CH_2Cl_2 molecule were disordered over three sites with occupancies 0.24/0.13/0.13. Also, all non-hydrogen atoms of the disordered CH_2Cl_2 molecules were restrained so that their U_{ij} components approximate to isotropic behavior. One of the phenyl rings (C7–C17) was also disordered over two sites with occupancies 0.51/0.49. All phenyl rings were slightly disordered and therefore the carbon atoms were fitted to a regular hexagon with C–C distance of 1.39 Å. In a crystal of **6** the solvent molecules were partially lost. One of the acetone molecules (C104–106, O4) was disordered over two sites with equal occupancies 0.5. In the second acetone molecule the C–O distance between C109 and O5 was fixed to 1.15 Å. Also, C109–C110 and C109–C111 bond lengths as well as anisotropic displacement parameters of C109, C110, C111, and O5 were set to be equal. Acetone carbon C105 was restrained so that its U_{ij} components approximate to isotropic behavior. The OH hydrogen atom in **6** was located from the difference Fourier map but constrained to ride on its parent atom, with $U_{iso} = 1.5$. Other hydrogens in all other structures were positioned geometrically and constrained to ride on their parent atoms, with C–H = 0.95–0.99 Å and U_{iso} = 1.2–1.5 U_{eq} (parent atom). The crystallographic details are summarized in the corresponding footnote‡ and Table S1†.

Computational details for DFT and TD-DFT calculations

The molecular coordinates used in the theoretical studies of (**1–6**) were obtained from the X-ray diffraction data and for the complex **4** $[(Au_2SPh)_2(1,4\text{-}PMe_2C_6H_4PMe_2)_2](PF_6)_2$ used as a model. This model was chosen to represent the experimental geometry by substituting from the X-ray diffraction structure the C_6H_5 rings by CH_3 group, to keep the computational cost feasible. In both the ground-state calculations and the subsequent calculations of the electronic excitation spectra, the B3LYP functional[48] as implemented in Gaussian[49] was used. The two first triplet transitions were calculated within the TDDFT formalism as implemented in Gaussian. The excitation energies were obtained at the density functional level using the time dependent perturbation theory approach (TDDFT), which is a DFT generalization of the

‡ Crystal data for **1**: $C_{90}H_{81}Au_4Cl_6P_4S_4$, M = 2415.23, colourless plate, 0.42 × 0.20 × 0.14 mm^3, triclinic, space group $P\bar{1}$, a = 16.7048(6), b = 16.7988(4), c = 16.8964(6) Å, α = 78.948(2), β = 68.399(2), γ = 79.416(2)°, V = 4293.4(2) Å^3, Z = 2, D_c = 1.868 g cm^{-3}, F_{000} = 2326, Mo-Kα radiation, λ = 0.71073 Å, T = 100(2)K, $2\theta_{max}$ = 55.0°, 76565 reflections collected, 19581 unique (R_{int} = 0.0448). Final *GooF* = 1.029, *R1* = 0.0478, *wR2* = 0.1223, *R* indices based on 15643 reflections with $I > 2\sigma(I)$ (refinement on F^2), 975 parameters, 9 restraints; *wR2* = 0.1380 (all data).Crystal data for **3**: $C_{72}H_{60}Au_2P_2S_2$, M = 1445.19, colourless plate, 0.46 × 0.17 × 0.14 mm^3, triclinic, space group $P\bar{1}$, a = 12.0886(3), b = 15.6319(4), c = 16.4470(4) Å, α = 96.8910(10), β = 99.389(2), γ = 100.712(2)°, V = 2976.45(13) Å^3, Z = 2, D_c = 1.613 g cm^{-3}, F_{000} = 1424, Mo-Kα radiation, λ = 0.71073 Å, T = 100(2)K, $2\theta_{max}$ = 55.0°, 51042 reflections collected, 13495 unique (R_{int} = 0.0490). Final *GooF* = 1.061, *R1* = 0.0332, *wR2* = 0.0616, *R* indices based on 10215 reflections with $I > 2\sigma(I)$ (refinement on F^2), 703 parameters, 0 restraints; *wR2* = 0.0709 (all data)Crystal data for **4**: $C_{162}H_{152}Au_8F_{24}O_6P_{12}S_4$, M = 4726.45, colourless block, 0.28 × 0.15 × 0.09 mm^3, triclinic, space group $P\bar{1}$, a = 14.7817(2), b = 15.1252(2), c = 20.7653(2) Å, α = 85.5220(10), β = 87.6520(10), γ = 60.9750(10)°, V = 4047.13(9) Å^3, Z = 1, D_c = 1.939 g cm^{-3}, F_{000} = 2264, Mo-Kα radiation, λ = 0.71073 Å, T = 100(2)K, $2\theta_{max}$ = 60.1°, 85127 reflections collected, 23604 unique (R_{int} = 0.0359). Final *GooF* = 1.077, *R1* = 0.0304, *wR2* = 0.0628, *R* indices based on 19166 reflections with $I > 2\sigma(I)$ (refinement on F^2), 1014 parameters, 56 restraints; *wR2* = 0.0676 (all data).Crystal data for **5**: $C_{43}H_{35}Au_2Cl_2F_6P_3S$, M = 1255.51, colourless block, 0.18 × 0.13 × 0.08 mm^3, triclinic, space group $P\bar{1}$, a = 12.4289(9), b = 14.5787(11), c = 14.9984(11) Å, α = 64.147(2), β = 81.263(2), γ = 71.597(3)°, V = 2320.3(3) Å^3, Z = 2, D_c = 1.797 g cm^{-3}, F_{000} = 1200, Mo-Kα radiation, λ = 0.71073 Å, T = 100(2)K, $2\theta_{max}$ = 55.3°, 30867 reflections collected, 10607 unique (R_{int} = 0.0413). Final *GooF* = 1.040, *R1* = 0.0527, *wR2* = 0.1304, *R* indices based on 7573 reflections with $I > 2\sigma(I)$ (refinement on F^2), 440 parameters, 148 restraints; *wR2* = 0.1440 (all data).Crystal data for **6**: $C_{217}H_{202}Au_8Cl_4F_{24}O_9P_{12}S_4$, M = 5627.20, colourless block, 0.26 × 0.12 × 0.10 mm^3, triclinic, space group $P\bar{1}$, a = 13.3559(14), b = 19.399(2), c = 21.065(3) Å, α = 85.626(11), β = 89.917(8), γ = 78.127(10)°, V = 5324.8(11) Å^3, Z = 1, D_c = 1.755 g cm^{-3}, F_{000} = 2736, Mo-Kα radiation, λ = 0.71073 Å, T = 100(2)K, $2\theta_{max}$ = 50.5°, 68671 reflections collected, 18105 unique (R_{int} = 0.0363). Final *GooF* = 1.072, *R1* = 0.0459, *wR2* = 0.1135, *R* indices based on 15295 reflections with $I > 2\sigma(I)$ (refinement on F^2), 1235 parameters, 9 restraints; *wR2* = 0.1226 (all data).

Hartree–Fock linear response (HF-LR) or random-phase approximation (RPA) method.[50] The TDDFT do not take into account the spin–orbit splitting. In all calculations, the Karlsruhe split-valence-quality basis sets augmented with polarization functions were used (SVP) for C, H atoms and TZVP for S and P atoms.[51] The Stuttgart effective core potential was used for Au.[52]

Results and discussion

Synthesis

Reactions of gold(I) phenyl-thiolate polymer with slight excess of the corresponding diphosphine afford binuclear neutral thiolate-diphosphine complexes **1–3** in excellent yield, see Scheme 1. This mild synthetic procedure[53] analogous to that commonly used in silver(I) chemistry[54] is an effective alternative to the widely employed metathetical reaction of phosphine gold(I) chloride and thiol in the presence of a deprotonation agent[11,15–17,24,55–57] or the reaction of a thiol with a Au(acac)(phosphine) complex, known as the "acac method".[2,56,58]

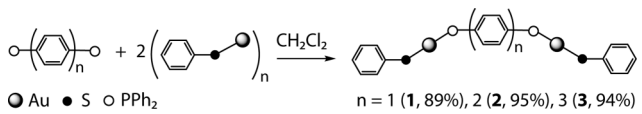

Scheme 1 Synthesis of the complexes **1–3**.

It has been already shown that neutral gold(I) thiolate-phosphine complexes can be effectively oxidized, *e.g.*, by Fc^+ or add cationic coordinatively unsaturated metal centers to form various polymetallic assemblies.[8,27,56,59] Indeed, treatment of the dimers **1–3** with stoichiometric amounts of $Fc(PF_6)$ resulted in formation of the tetranuclear dicationic complexes $[(Au_2SPh)_2(PPh_2(C_6H_4)_nPPh_2)_2](PF_6)_2$ (n = 1 (**4**), 2 (**5**), 3 (**6**)), Scheme 2, method **C**. However, this preparative route was found to be ineffective as the purification workup required tedious recrystallization and gave the title compounds in relatively low yields. Therefore we investigated other synthetic options, namely depolymerization of $(AuSPh)_\infty$ with cationic diphosphine complexes $[Au_2(PPh_2(C_6H_4)_nPPh_2)_2](PF_6)_2$ (n = 1, 2, 3) or addition of the labile species $[\{Au(SC_4H_8)\}_2PPh_2(C_6H_4)_nPPh_2](PF_6)_2$ (n = 1, 2, 3) generated *in situ* to the dimers **1–3** (Scheme 2, methods **A** and **B**). These protocols afforded the same tetragold complexes **4–6** obtained *via* the oxidation process but in considerably higher yields (66–91%).

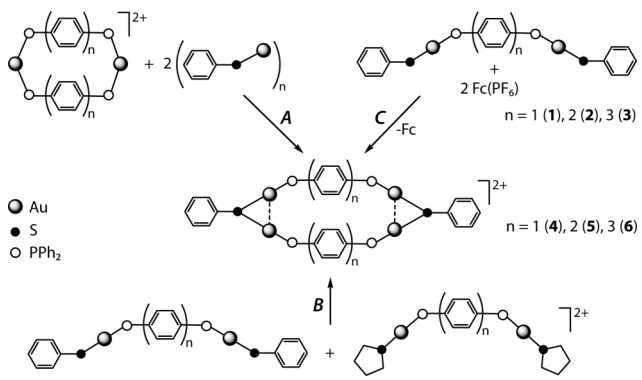

Scheme 2 Synthesis of the complexes **4–6**.

Elemental analysis of **1–3** and NMR spectroscopic data of these complexes are compatible with the structure suggested in Scheme 1. The 1D ^1H and COSY spectra of **1–3** (see Figures S1–S3, Supporting Information†) display well separated high field signals of *meta*-(*ca.* 7.1 ppm) and *para*-(*ca.* 7.0 ppm) protons of the phenylthiolate ligand together with the doublet of *ortho*-protons (*ca.* 7.6 ppm) in the low field part of the spectra. The latter signals are masked by the resonances of the phosphine ligand protons in the 1D spectrum but are clearly resolved in the corresponding 2D COSY spectra. Quite expectedly the positions of these signals are nearly identical in **1–3** because of the minor effect of the number of phosphine ligand spacers onto shielding of the thiolate ligand protons. Aromatic protons of the phosphine ligands generate a poorly resolved set of signals in the 7.8–7.45 ppm range that correlates well with the ^1H spectroscopic data obtained for closely analogous binuclear gold(I) alkynyl-phosphine complexes.[32,33] The relative intensities of the thiolate and phosphine proton signals in the ^1H NMR spectra are in complete agreement with the suggested molecular structure.

X-ray crystallographic study of **1–3** revealed that the structure shown in Scheme 1 is retained in the crystal cell. The solid state structures of these compounds together with selected structural parameters are shown in Fig. 1, 2, S4†. Poor diffraction of the crystals of **2** didn't allow for high-quality refinement, therefore these crystallographic data are used as supporting material only. The complexes **2** and **3** exist in crystalline state as independent isolated molecules and do not show any intermolecular aurophilic contacts typical for gold(I) complexes.[60,61] In contrast to these structural patterns the solid state structure of **1** shows the intermolecular Au-Au contacts (3.190 Å) to form infinite "zig-zag" chains as shown in Fig. 1. Local environment of gold(I) ions in **1–3** features essentially linear P-Au-S geometry with the Au-S and Au-P distances in the ranges 2.29–2.31 and 2.25–2.27 Å, respectively. It is worth noting that aurophilic bonding in the solid state structure of **1** does not affect the molecular structural parameters within the gold(I) environment.

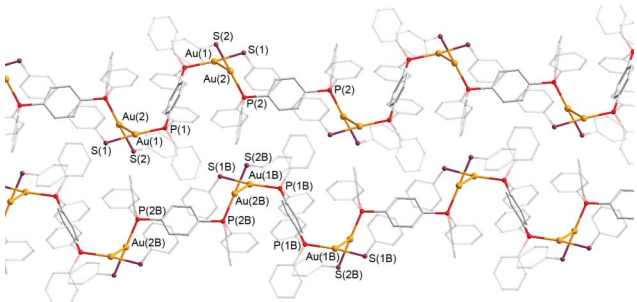

Fig. 1 Solid state structure of **1**. Selected interatomic distances (Å) are: Au(1)–P(1) 2.271(2), Au(1)–S(1) 2.310(2), Au(2)–P(2) 2.257(2), Au(2)–S(2) 2.302(2), Au(1)–Au(2) 3.1960(4), Au(1B)–P(1B) 2.267(2), Au(1B)–S(1B) 2.309(2), Au(2B)–P(2B) 2.260(2), Au(2B)–S(2B) 2.308(2), Au(1B)–Au(2B) 3.1901(5). Selected bond angles (°) are: P(1)–Au(1)–S(1) 175.03(7), P(2)–Au(2)–S(2) 179.17(6), P(1B)–Au(1B)–S(1B) 173.06(7), P(2B)–Au(2B)–S(2B) 179.35(7).

Elemental analysis and ESI mass-spectroscopic data (Figures S5–S7†) for the complexes **4–6** indicate that these molecules contain four gold(I) ions, which coordinate two diphosphine and two thiolate ligands. The most probable molecular structure

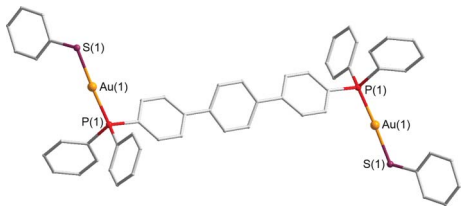

Fig. 2 Solid state structure of **3**. One of two independent molecules is shown. Selected interatomic distances (Å) are: Au(1)–P(1) 2.251(1), Au(1)–S(1) 2.290(1), Au(2)–P(2) 2.261(1), Au(2)–S(2) 2.299(1). Selected bond angles (°) are: P(1)–Au(1)–S(1) 176.64(4), P(2)–Au(2)–S(2) 179.20(4).

compatible with this stoichiometry is shown in Scheme 2. The 1D and COSY proton NMR spectra of **4–6** (see Experimental and

Figs. S8–S10†) are in complete agreement with the presence of one thiolate and one phosphine ligand per two Au(I) ions in the dicationic molecule. In contrast to **1–3** the thiolate ligand in **4–6** occupies a bridging position between two cations that causes low field shift of the phenyl-thiolate resonances and their overlapping with the signals of the phosphine ligands in 1D spectra. Nevertheless, correlations observed in the 2D COSY spectra allow for differentiation of two groups of multiplets and their assignment to corresponding ligands.

Compounds **4–6** were also studied using X-ray crystallography. Their solid state structures are shown Fig. 3–5. In contrast to **1–3** none of the **4–6** complexes crystallize in their molecular form due to formation of supramolecular aggregates, the structures of which are dictated by a network of aurophilic interactions. In the solid state structures of **4–6** it is possible to isolate a common structural motif (Chart 1), which consists of four gold(I) ions and two thiolate ligands brought together by Au-S bonding and aurophilic interactions.

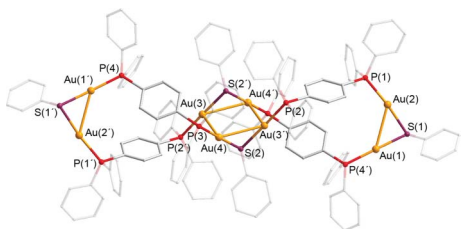

Fig. 3 Solid state structure of the complex **4**. Counterions (PF_6^-) omitted for clarity. Selected interatomic distances (Å) are Au(1)–S(1) 2.340(1), Au(1)–Au(2) 3.0130(2), Au(2)–P(1) 2.268(1), Au(2)–S(1) 2.336(1), Au(3)–P(2) 2.272(1), Au(3)–S(2) 2.340(1), Au(3)–Au(4′) 3.0847(2), Au(3)–Au(4) 3.1505(2), Au(4)–P(3) 2.265(1), Au(4)–S(2) 2.339(1), Au(4)–Au(3′) 3.0846(2). Selected bond angles (°) are: P(1)–Au(2)–S(1) 171.36(4), P(4′)–Au(1)–S(1) 176.91(4), P(2)–Au(3′)–S(2) 176.89(4), P(3)–Au(4)–S(2) 176.97(4).

These gold(I) ions additionally coordinate four other ligands thus accomplishing the corresponding structural pattern. This structural motif was revealed earlier in a good deal of gold(I) thiolate complexes containing monophosphine and some bidentate ligands of various nature,[27,30,53,57,62] but it was mainly presented as an isolated structural unit because of saturation of the metal ion vacancies and ligand coordination functions. In a very few crystal structures containing bidentate thiols this unit was found to be incorporated into polymeric chains.[6,63] In the case of **4** formation of this structural pattern affords the $[PhSAu_2(Ph_2PC_6H_4PPh_2)_2\{Au_4$

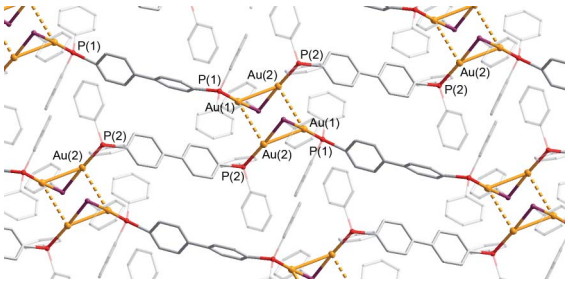

Fig. 4 Solid state structure of the complex **5**. Counterions (PF_6^-) omitted for clarity. Selected interatomic distances (Å) are Au(1)–P(1) 2.267(3), Au(1)–S(1) 2.333(2), Au(1)–Au(2) 3.0368(5), Au(1)–Au(2) interchain 3.4373(6), Au(2)–P(2) 2.269(3), Au(2)–S(1) 2.336(2). Selected bond angles (°) are: P(1)–Au(1)–S(1) 177.1(1), P(2)–Au(2)–S(1) 176.65(9).

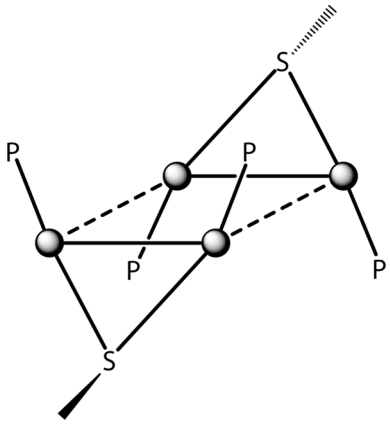

Chart 1 Schematic view of the $\{Au_4P_4(\mu\text{-}SPh)_2\}$ unit found in **4–6**.

$(SPh)_2\}(Ph_2PC_6H_4PPh_2)_2Au_2SPh]^{4+}$ an isolated tetracation shown in Fig. 3. This structure can be considered as a result of dimerization of the molecules shown in Scheme 2. Formation of the $\{PhSAu_2P_2\}$ and $\{Au_4(SPh)_2\}$ structural patterns does not change the linear geometry about the gold(I) centers, the P-Au-S angles equal to 171.4° and 176.9° in the digold and 177.0° in the tetragold fragments. The Au-Au distances found in the solid state structure of **4** (3.0130(2) Å in $\{Au_2\}$ and 3.0846(2), 3.1505(2) Å in $\{Au_4\}$ fragments) fall in the range of typical aurophilic contacts.[60,61]

In the case of **5** the $\{PhSAuPh_2P(C_6H_4)_2PPh_2Au\}$ units form infinite chains, which in turn are bound to each other through formation of the $\{Au_4(SPh)_2\}$ fragments. These fragments cross-link the chains to give the 2D supramolecular structure shown in Fig. 4. The Au-Au distances bridged by the thiolate ligands (inside the chains) are substantially shorter (3.0368(5) Å) compared to the unsupported Au-Au contacts between the chains (3.4373(6) Å), which still could be considered as weak aurophilic bonds. Linear geometry about the gold(I) centers remains unchanged to give the values of P-Au-S angles very close to 177°.

The solid state structure of **6** (Fig. 5) displays another way of intermolecular aurophilic bonding to give an infinite double stranded chain formed by the molecular $[(PhSAu_2)(PPh_2(C_6H_4)_3PPh_2)_2(Au_2SPh)]^{2+}$ units, which are bound to each other by unsupported aurophilic contacts. These contacts give rise to formation of the $\{Au_4(SPh)_2\}$ units, which links together the monomeric units of this chain. It is interesting that

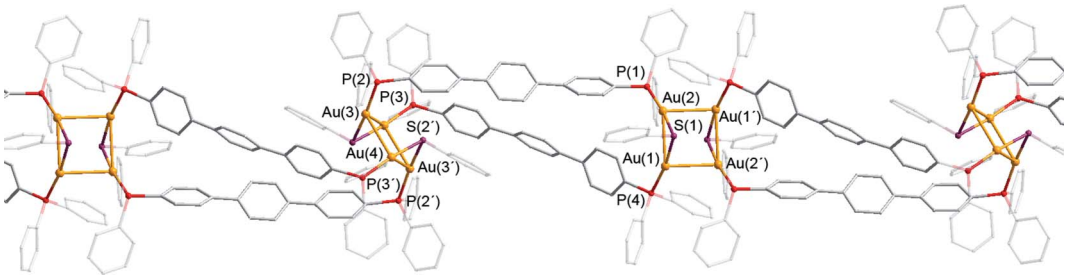

Fig. 5 Solid state structure of the complex **6**. Counterions (PF_6^-) omitted for clarity. Selected interatomic distances (Å) are Au(1)–P(4) 2.275(2), Au(1)–S(1) 2.350(2), Au(1)–Au(2′) 3.0169(5), Au(1)–Au(2) 3.0806(6), Au(2)–P(1) 2.276(2), Au(2)–S(1) 2.350(2), Au(2)–Au(1′) 3.0168(5), Au(3)–P(2) 2.275(2), Au(3)–S(2) 2.352(2), Au(3)–Au(4) 3.0391(6), Au(3)–Au(4′) 3.0767(6), Au(4)–P(3′) 2.277(2), Au(4)–S(2′) 2.358(2), Au(4)–Au(3′) 3.0767(6). Selected bond angles (°) are: P(1)–Au(2)–S(1) 171.69(8), P(4)–Au(1)–S(1) 171.40(7), P(2)–Au(3)–S(2) 170.38(8), P(3)–Au(4)–S(2) 173.91(9).

in contrast to the structures of **4** and **5** the unsupported Au–Au contacts (3.039 and 3.017 Å) are shorter compared to those bridged by thiolate ligands (3.077 and 3.081 Å).

Photophysics

Solution studies

The UV/vis spectra of the complexes **1–6** display absorption bands between 237 and 305 nm (Figure S11†). The similar patterns have been observed for other complexes with oligophenylene spacers.[32,33,64] Absorption bands near 300 nm have been attributed to the promotion of an electron from σ(Au-P) orbital to the empty π* antibonding orbital located at the bridging phenylene groups. Higher energy absorptions (below 250 nm) have been assigned to the IL transitions. In addition, compound **6** displays an absorption shoulder at 328 nm. Absorption bands at similar energies have been mentioned in previous works[9,12,65] for either charge transfer processes (S"Au) or the presence of gold · · · gold interactions which, according to mass-spectroscopic measurements, are probably retained in solution in complexes **4–6**, as shown in Scheme 2.

All the complexes are weakly luminescent in the fluid medium both at 298 and 77 K. The **2**, **5** and **3**, **6** couples of complexes show very similar excitation and emission patterns in dichloromethane solution both at room and low temperature, although the diphosphine $Ph_2P(C_6H_4)_3PPh_2$ displays dual emission in dichloromethane solution at 298 K (see Table 1 and Fig. 6). The room temperature emission spectra for these couples of complexes display broad bands centered at 390 nm and 375 nm, respectively. Considerable magnitude of Stokes shift together with the luminescence lifetime in microsecond domain point to a phosphorescent nature of the emission.

Upon cooling the solutions down to 77 K the emission bands are substantially red shifted, *ca.* 100 nm (500 cm^{-1}) for **2**, **5** and 170 nm (800 cm^{-1}) for **3**, **6**, and transformed into the well resolved vibronically structured bands with vibronic progression of *ca.* 1200 cm^{-1}, typical for the excited states of aromatic systems. The same phenomenon is observed for the free diphosphines, although the vibronic structure is not so clearly resolved. Luminescence

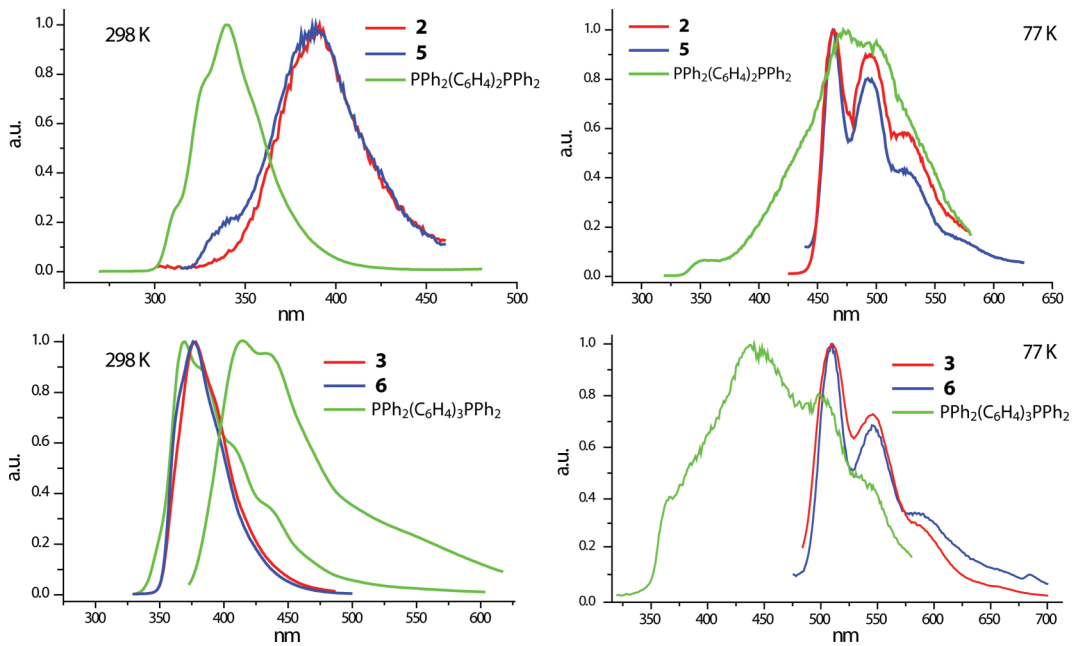

Fig. 6 Emission spectra of the complexes **2**, **5** and **3**, **6** and the diphosphines $Ph_2P(C_6H_4)_nPPh_2$ ($n = 2, 3$) in dichloromethane at 298 K and 77 K.

Table 1 Absorption, DRUV, excitation and emission data of diphosphine ligands and compounds **1–6**[a]

	298 K			77 K	
Compound	λ_{abs}/nm ($10^{-5}\varepsilon$, l mol^{-1} cm)	λ_{exc}/nm[b]	λ_{em}/nm[b] (τ[c], μs)	λ_{exc}/nm[b]	λ_{em}/nm[b]
Solution					
$Ph_2PC_6H_4PPh_2$		310	365	275, 315	450
1	238 (1.12), 254 (0.67), 277sh (0.42), 305sh (0.15)	241, 330	385[d] 525[d]	(307–370)[f]	485
4	237 (14.1), 253 (6.8), 279sh (5.3), 303(sh) (2.7)	240, 320	380	350[e,d]	487
				270[e], 350	[387, 407, 430][e]
$Ph_2P(C_6H_4)_2PPh_2$		250, 285	340	270, 340	485
2	238(1.85), 253(0.94), 279sh (0.62), 304sh (0.41)	241	390	270, 345	463, 495, 523
5	237(4.5), 253(2.2), 281sh (1.6), 304sh (0.91)	240, 330	390	270, 340	463, 495, 524
$Ph_2P(C_6H_4)_3PPh_2$		310, 360	370, 420	300, 350	445
3	238 (6.9), 241 (3.0), 281sh (1.74), 305sh (0.46)	240, 310	377	276, 362	510, 545, 590
6	238 (3.5), 253 (1.7), 278sh (1.2), 304sh (0.76), 328sh (0.19)	(280–330), 350	375	275, 343	510, 545, 586
Solid phase DRUV (λ_{max}/nm)					
$Ph_2PC_6H_4PPh_2$	295	270, 370, 400 360, 400	445, 470	330, 405	480
1	330	260	453 (116)	(296–417)	462
4	300			400	515
$Ph_2P(C_6H_4)_2PPh_2$	308	370	470	335, 370	430, 500
2	310	370	500 (54)	275, 370	510
5	305	330	470, 500, 535 (49)	270, 330, 370	470, 500, 535
$Ph_2P(C_6H_4)_3PPh_2$	315	370, 440 270, 405	450, 490	275, 390	480
3	317	357, 396	505 (1030)	360	490, 520, 560
6	320	375	420 (2141)	350, 380	510, 550, 590

[a] Degassed CH_2Cl_2 solution. [b] In the excitation spectra comma separated values indicate more than one maximum of excitation for the same emission. In the emission spectra comma separated values in the same line belong to a structured band. Emission maxima belonging to different maxima for the same compound are shown in different lines. [c] Coefficient of determination (R^2) to a first order exponential function is 0.99, except for **1** and **3** in solid phase, which are 0.98 and 0.95 respectively. [d] The same excitation maximum appears in both emissions, but the intensity depends on the excitation band. [e] Most intense band. [f] Maximum not well defined.

thermochromism has been described in the literature and the bathochromic shift of the emission upon lowering temperature have been attributed to thermal contraction that occurs upon cooling, which leads to a reduction in the band-gap energy.[66] From this data it seems reasonable to suggest substantial contribution of the diphosphine orbitals into the molecular ones, which are responsible for the luminescence originating either from the intraligand transitions (more or less modified by coordination to gold) or charge transfer processes.

Behavior of the **1**, **4** relatives containing only one phenylene spacer between the phosphorus coordinating centers is more complicated (Fig. 7). Both complexes display dual emission generated by two emissive excited states at room temperature for **1** and at low temperature for **4**. In the latter case vibronicallystructured emission (387, 407, 430 nm) as well as excitation (270, 350 nm) spectra fit well the emission discussed above for the pairs of complexes **2**, **5** and **3**, **6** although the shape of the emission at lower energy (487 nm) displays more similarity with that of the free diphoshine and with the emission shown by **1** (485 nm) at 77 K. This red shifted component (487 nm) originates from 350 nm excitation band and could be assigned to IL (diphosphine) transitions or charge transfer (CT) processes involving either two ligands (thiolate and diphosphine) or the gold center and one (or both) of the ligands. In contrast, complex **1** gives two emission

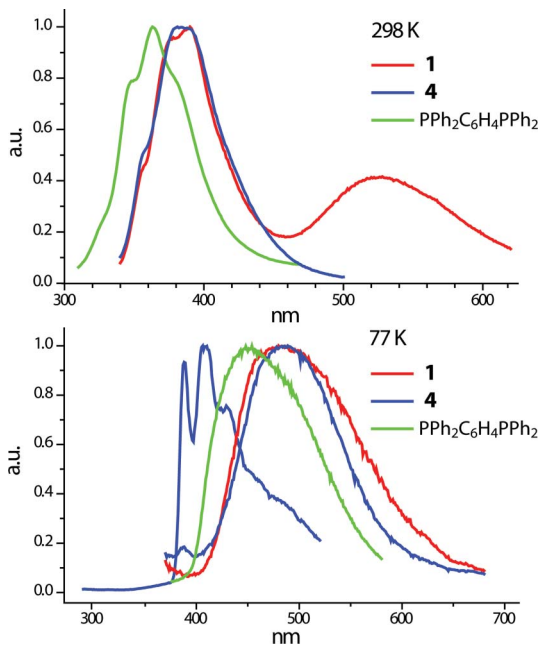

Fig. 7 Emission spectra of the complexes **1**, **4** and the diphosphine $Ph_2PC_6H_4PPh_2$ in dichloromethane at 298 K (top) and 77 K (bottom).

bands at room temperature at 385 and 525 nm, which are not resolved in the excitation spectrum. Both emissions are observed upon excitation at any of the two excitation maxima (see Table 1), but the emission at higher energies is more intense upon excitation at higher energy component and excitation at 330 nm leads to more intense emission at 525 nm. The shorter wavelength component of the emission looks similar to the emission bands displayed by **4** and free diphosphine under the same conditions and could be associated IL (diphosphine) transitions modified by coordination to gold, whereas the band at 525 nm could be related to that at lower energies for **4** at 77 K, mentioned above.

Dual emission from different triplet states has been previously described.[67] The presence of only one emission in the case of **4** at room temperature may be explained by quenching processes for the lower energy emission (the most intense at low temperature), which are expected to be more effective at higher temperature. Complex **1** displays dual emission at room temperature. At both temperatures the emission covers a wide range of about 300 nm. As quenching processes are expected to be more effective with raising the temperature we propose coupling of both states upon lowering the temperature. One of the most important consequences from the analysis of the data is that the presence (in **4–6**) or absence (in **1–3**) of intramolecular aurophilic bonding does not substantially affect the emission parameters of these complexes.

Solid state studies

DRUV spectra have been recorded for **1–6** and for the free diphosphines (Table 1, see also Figure S12†). The complexes display one broad band centered between 300 and 330 nm. These data are consistent with those observed in solution and aggregation and the solid state seems to have no effect on the absorption characteristics of the compounds under study.

Except compound **4**, which is not emissive in the solid state at room temperature, the solid samples are luminescent both at room temperature and at 77 K. The emission lifetimes, which are in the microsecond domain, are indicative of triplet manifold luminescence. In general, the position of the emission maxima in solid state at 298 K emission are red shifted compared to the values found in solution. A small red shift (in most cases less than 30 nm) was also observed in the low temperature solid state spectra, compared with those at 298 K that is in line with solution thermochromism.[66] Complexes **3** and **6** show vibronic progression at 77 K (Table 1), similar to that observed in solution (Fig. 8). Once again, it has to be noted that the free diphosphine ligands display very similar trends in their spectral patterns with those of the complexes. Therefore it is possible to propose a substantial contribution of the ligand orbitals among those involved in the emissive excited states.

We can then conclude that the emissive properties of the complexes **1–6**, either in solution or in the solid state, seem to be mainly determined by the IL or CT electronic transitions with substantial contribution of the diphosphine ligand orbitals. This assignment is in sharp contrast with interpretation of the data obtained earlier for the gold(I) thiolate complexes containing mono-[11,12,15–17,57,68] and diphosphine[8,16,24,31,56] ligands. As shown in a recent review[9] on this topic the main contribution to the luminescence of the complexes of this type comes from LMCT (S→Au) excited states. In some cases, particularly for the complexes which tend to form aurophilic bonding, the contribution from (LMMCT, S→(Au···Au))[11,24,56] as well as the metal centered (MC) transitions[12,15,56,68] may be also observed. In accord with this assignment none of the gold(I) thiolate-phosphine complexes studied earlier displays vibronically structured emission (found for **1–6**), neither in solution nor in solid state. Another characteristic feature of the emission observed for the complexes containing diphosphines with polymethylene spacers, Ph_2P-$(CH_2)_n$-PPh_2 (n = 1–5), is independence of emission characteristics on the structure of the phosphine ligands,[24,31] *i.e.* their contribution into the excited states and observed luminescence is absent or negligible. The only exclusion can be exemplified by the calculations of the electronic structure of dppm(Au-S-C_6H_4-(2-NH_2))$_2$ complex, where emissive excited states are related to the LUMO located onto gold(I) ions and phosphorus atoms, representing Au···Au interaction and Au–P bonding.[56] The family of **1–6** differs from the Au(I)-thiolate phosphine complexes mentioned above by the presence of conjugated aromatic spacers between (P–Au) coordination

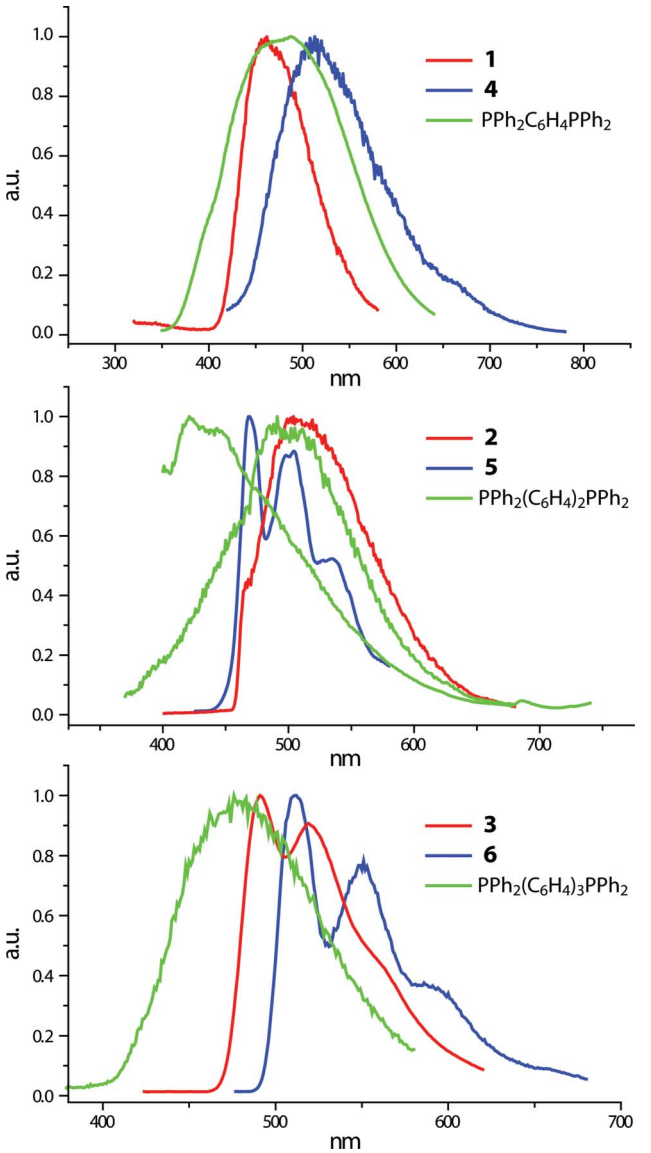

Fig. 8 The solid state emission spectra of complexes **1–6** and the corresponding diphosphines $PPh_2(C_6H_4)_nPPh_2$ (n = 1–3) at 77 K.

Table 2 Data for the first singlet→triplet transition for complexes **1–6**

Complex	λ_T (nm)[a]	Transition
1	488	HOMO (193) → LUMO (194)
2	496	HOMO (213) → LUMO (214)
3	502	HOMO (233) → LUMO (234)
4	459	HOMO-1 (399) → LUMO+1 (402)
5	862	HOMO-1 (183) → LUMO (185)
6	446	HOMO-1 (407) → LUMO (409)

[a] λ_T = Calculated absorption wavelength.

centers. These observations point to unusually important effect of this conjugation onto luminescence of these species. In order to verify this point we have carried out the calculations for the complexes under investigation.

Computational results

DFT calculations were performed in order to elucidate the electronic structure of complexes **1–6**, to check the contribution of each part of the molecule to the frontier orbitals involved in the transitions responsible for the photoluminescence. As the lifetime measurements point to a phosphorescent nature of the observed emissions, the mechanism of the luminescence is considered to involve a spin-forbidden transition, and thus the first singlet–triplet transitions were calculated using the TDDFT methods. These transitions are assumed to correspond to the emission observed upon excitation at 340–370 nm. Calculations do not evaluate the spin–orbit splitting. Thus, only a proposal but not a complete assignment can be made. The data obtained are summarized in Table 2 and shown in Fig. 9. For the complexes **1–6** the first singlet–triplet transition is related to the transitions between the HOMO or HOMO-1 and the LUMO orbitals. The analysis of the active orbitals shows that for all the complexes except **5**, HOMO and HOMO-1 are mainly located at the phenyl thiolate ligand with a small contribution from the gold center, whereas for **5** HOMO is mainly located at the diphosphine and LUMO – at the phenylthiolate with the contribution of one of the gold atoms.

The predicted energy values for the excitations show that the theoretical values appear at lower energy than those obtained experimentally. It should be pointed out, however, that TDDFT calculations were mainly performed on the isolated molecules and ignored the aggregation contribution in the solid state.[50,60,69] In the case of **5** the $\{PhSAuPh_2P(C_6H_4)_2PPh_2Au\}$ units form infinite chains. Another interesting aspect is that the complexes show broad and vibronically structured bands. However, it has been shown that DFT calculations could be used to describe large systems, and the TDDFT approach allows for assignment of the excitations, which lead to emission.[70]

In agreement with the above calculations, we propose the assignment of the emission as derived from the ligand to ligand charge transfer processes, namely from phenyl thiolate ligand orbitals with the contribution from the gold center (LM') to the phenylene spacers of the diphosphine [LM'-LCT: PhSAu → Ph(spacer)] for the **1–4** and **6** complexes, and to the LLM'CT: diphosphine → SPhAu in **5**. It is worth noting that in the both cases the phenylene spacers of the diphosphine ligands play a key role in these transitions.

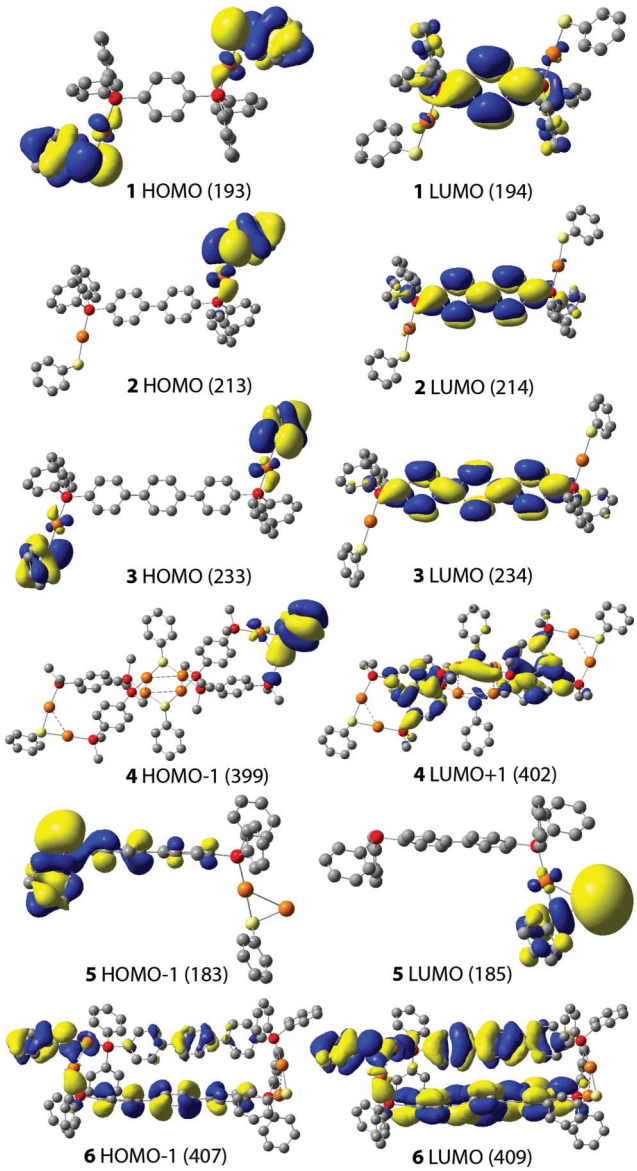

Fig. 9 The frontier molecular orbitals responsible for singlet–triplet transitions in the complexes **1–6**.

Two conclusions may be deduced from the DFT and TDDFT results. The first one is that a gold(I)–gold(I) interaction is not a necessary condition for luminescence in the gold–phosphine complexes. Further, this theoretical study also indicates that the presence of a gold(I)–gold(I) contact does not significantly perturb the luminescence parameters in this series of complexes. This is in complete agreement with the general photophysical behavior of **1–6** (see Table 1), where there is no correlation between intramolecular aurophilic interactions and the energy or shape of the bands observed in the excitation and emission spectra. The luminescence spectra of complexes **4–6**, which also have gold(I)–gold(I) interactions in the solid state, are not affected by the contributions of the σ and σ* molecular orbitals (formed by overlap of filled dz^2 orbitals on Au) as long as the highest occupied molecular orbital remains sulfur in character.

Conclusions

We present a series of novel gold(I)–thiolate complexes based on the diphoshosphine ligands with oligophenylene spacers, PPh_2-$(C_6H_4)_n$-PPh_2 ($n = 1, 2, 3$). The dinuclear species, $[(AuSPh)_2(PPh_2$-$(C_6H_4)_n$-$PPh_2)]$ (**1–3**) are effectively converted into their tetranuclear cationic derivatives of the general formula $[(Au_2SPh)_2(PPh_2$-$(C_6H_4)_n$-$PPh_2)_2](PF_6)_2$ (**4–6**) using different synthetic pathways. X-ray crystallographic studies have been performed for all the compounds, which show that in the solid state the tetranuclear clusters do not crystallize in their molecular forms found in solution due to the aurophilic aggregation, the structural topology of which is unique for each of the complexes studied. The detailed photophysical measurements reveal luminescence of all the species both in the solid state and solution. The theoretical calculations of the electronic structures suggest that thiolate and diphosphine intraligand charge transfer processes are of primary responsibility for the emissions. Moreover, the presence or absence of aurophilic interactions does not have any detectable effect on the luminescent behavior. This origin of luminescence in **1–6** is very different from the thiolate to gold charge transfer transitions, usually reported for the gold-thiolate species. The results obtained clearly indicate an important role that the phenylene spacers of the diphosphines play in the unusual photophysical behavior of these complexes.

Acknowledgements

Financial support from the Academy of Finland (I.O.K.), Russian Foundation for Basic Research (grants 09-03-12309-CSIC-a and 09-03-12309) is gratefully acknowledged. We also thank the Dirección General de Investigación Científica y Técnica (CTQ2007-67273-C02-01), the CSIC/Russian Foundation for Basic Research (RFBR) (N 2008RU0065) for financial support and to the Supercomputing Center of Galicia (CESGA-CSIC) for providing Access to the FINIS TERRAE System.

Notes and references

1 R. M. Davila, A. Elduque, T. Grant, R. J. Staples and J. P. J. Fackler, *Inorg. Chem.*, 1993, **32**, 1749–1755.
2 J. Vicente, M.-T. Chicote, P. González-Herrero and P. G. Jones, *J. Chem. Soc., Dalton Trans.*, 1994, 3183–3187.
3 J. Vicente, M.-t. Chicote and C. Rubio, *Chem. Ber.*, 1996, **129**, 327–330; J. C. Deaton and H. R. Luss, *J. Chem. Soc., Dalton Trans.*, 1999, 3163–3167; M. E. Olmos, in *Modern Supramolecular Gold Chemistry*, ed. A. Laguna, Wiley-VCH, Weinheim, 2008, pp. 295–346; A.-X. Zheng, Z.-G. Ren, L.-L. Li, H. Shang, H.-X. Li and J.-P. Lang, *Dalton Trans.*, 2011, **40**, 589–596; A. Ilie, C. I. Rat, S. Scheutzow, C. Kiske, K. Lux, T. M. Klapotke, C. Silvestru and K. Karaghiosoff, *Inorg. Chem.*, 2011, **50**, 2675–2684.
4 M. C. Gimeno, P. G. Jones, A. Laguna, M. Laguna and R. Terroba, *Inorg. Chem.*, 1994, **33**, 3932–3938; B.-C. Tzeng, A. Schier and H. Schmidbaur, *Inorg. Chem.*, 1999, **38**, 3978–3984.
5 O. Crespo, M. C. Gimeno, P. G. Jones, B. Ahrens and A. Laguna, *Inorg. Chem.*, 1997, **36**, 495–500; J. M. Lopez-de-Luzuriaga, A. Sladek, A. Schier and H. Schmidbaur, *Inorg. Chem.*, 1997, **36**, 966–968; D. W. Allen, R. Berridge, N. Bricklebank, E. Cerrada, M. E. Light, M. B. Hursthouse, M. Laguna, A. Moreno and P. J. Skabara, *J. Chem. Soc., Dalton Trans.*, 2002, 2654–2659.
6 H. Ehlich, A. Schier and H. Schmidbaur, *Inorg. Chem.*, 2002, **41**, 3721–3727.
7 W. J. Hunks, M. C. Jennings and R. J. Puddephatt, *Inorg. Chem.*, 2002, **41**, 4590–4598.
8 J. Chen, A. A. Mohamed, H. E. Abdou, J. A. K. Bauer, J. P. J. Fackler, A. E. Bruce and M. R. M. Bruce, *Chem. Commun.*, 2005, 1575–1577.
9 E. R. T. Tiekink and J.-G. Kang, *Coord. Chem. Rev.*, 2009, **253**, 1627–1648.
10 X. He and V. W.-W. Yam, *Inorg. Chem.*, 2010, **49**, 2273–2279.
11 J. M. Forward, D. Bohmann, J. P. J. Fackler and R. J. Staples, *Inorg. Chem.*, 1995, **34**, 6330–6336.
12 B.-C. Tzeng, C.-K. Chan, K.-K. Cheung, C.-M. Che and S.-M. Peng, *Chem. Commun.*, 1997, 135–136.
13 R. E. Bachman, S. A. Bodolosky-Bettis, S. C. Glennon and S. A. Sirchio, *J. Am. Chem. Soc.*, 2000, **122**, 7146–7147; E. J. Fernandez, A. Laguna, J. M. Lopez-de-Luzuriaga, M. Monge, M. Montiel, M. E. Olmos, R. C. Puelles and E. Sanchez-Forcada, *Eur. J. Inorg. Chem.*, 2007, 4001–4005; V. W.-W. Yam and E. C.-C. Cheng, *Top. Curr. Chem.*, 2007, **281**, 269–309; J. M. López-de-Luzuriaga, in *Modern Supramolecular Gold Chemistry*, ed. A. Laguna, Wiley-VCH, Weinheim, 2008, pp. 347–402; R. E. Bachman and S. A. Bodolosky-Bettis, *Z. Naturforsch.*, 2009, **64b**, 1491–1499; S. M. Bessey, M. Aghamoosa, G. S. P. Garusinghe, A. Chandrasoma, A. E. Bruce and M. R. M. Bruce, *Inorg. Chim. Acta*, 2010, **363**, 279–282; E. J. Fernandez, A. Laguna, J. M. Lopez-de-Luzuriaga, M. Monge and E. Sanchez-Forcada, *Dalton Trans.*, 2011, **40**, 3287–3294.
14 Y.-A. Lee and R. Eisenberg, *J. Am. Chem. Soc.*, 2003, **125**, 7778–7779.
15 B.-C. Tzeng, H.-T. Yeh, Y.-C. Huang, H.-Y. Chao, G.-H. Lee and S.-M. Peng, *Inorg. Chem.*, 2003, **42**, 6008–6014.
16 S. Y. Ho, E. C.-C. Cheng, E. R. T. Tiekink and V. W.-W. Yam, *Inorg. Chem.*, 2006, **45**, 8165–8174.
17 J.-G. Kang, H.-K. Cho, C. Park, S.-S. Yun, J.-K. Kim, G. A. Broker, D. R. Smyth and E. R. T. Tiekink, *Inorg. Chem.*, 2007, **46**, 8228–8237.
18 Q.-F. Sun, T. Kwok-Ming Lee, P.-Z. Li, L.-Y. Yao, J.-J. Huang, J. Huang, S.-Y. Yu, Y.-Z. Li, E. C.-C. Cheng and V. W.-W. Yam, *Chem. Commun.*, 2008, 5514–5516.
19 S.-H. Cha, J.-U. Kim, K.-H. Kim and J.-C. Lee, *Chem. Mater.*, 2007, **19**, 6297–6303.
20 C.-H. Li, S. C. F. Kui, I. H. T. Sham, S. S.-Y. Chui and C.-M. Che, *Eur. J. Inorg. Chem.*, 2008, 2421–2428.
21 V. W.-W. Yam and E. C.-C. Cheng, *Gold Bull.*, 2001, **34**, 20–23; P. D. Jadzinsky, G. Calero, C. J. Ackerson, D. A. Bushnell and R. D. Kornberg, *Science*, 2007, **318**, 430–433; E. J. Fernández and M. Monge, in *Modern Supramolecular Gold Chemistry*, ed. A. Laguna, Wiley-VCH, Weinheim, 2008, pp. 131–180; N. Lardiés, I. Romeo, E. Cerrada, M. Laguna and P. J. Skabara, *Dalton Trans.*, 2007, 5329–5338.
22 C. F. I. Shaw, *Chem. Rev.*, 1999, **99**, 2589–2600; E. A. Pacheco, E. R. T. Tiekink and M. W. Whitehouse, in *Gold Chemistry*, ed. F. Mohr, Wiley-VCH, Weinheim, 2009, pp. 283–319; K. P. Bhabak, B. J. Bhuyan and G. Mugesh, *Dalton Trans.*, 2011, **40**, 2099–2111.
23 V. W.-W. Yam, C.-K. Li and C.-L. Chan, *Angew. Chem., Int. Ed.*, 1998, **37**, 2857–2859; M. A. Mansour, W. B. Connick, R. J. Lachicotte, H. J. Gysling and R. Eisenberg, *J. Am. Chem. Soc.*, 1998, **120**, 1329–1330; X. He, F. Herranz, E. C.-C. Cheng, R. Vilar and V. W.-W. Yam, *Chem.–Eur. J.*, 2010, **16**, 9123–9131.
24 V. W.-W. Yam, C.-L. Chan, C.-K. Li and K. M.-C. Wong, *Coord. Chem. Rev.*, 2001, **216-217**, 173–194.
25 L. G. Kuz'mina, T. V. Baukova, A. V. Churakov, V. S. Kuz'min and N. V. Dvortsova, *Rus. J. Coord. Chem.*, 1997, **23**, 279–288.
26 W. J. Hunks, M. C. Jennings and R. J. Puddephatt, *Inorg. Chim. Acta*, 2006, **359**, 3605–3616.
27 J. Chen, T. Jiang, G. Wei, A. A. Mohamed, C. Homrighausen, J. A. K. Bauer, A. E. Bruce and M. R. M. Bruce, *J. Am. Chem. Soc.*, 1999, **121**, 9225–9226; A. A. Mohamed, J. Chen, A. E. Bruce, M. R. M. Bruce, J. A. K. Bauer and D. T. Hill, *Inorg. Chem.*, 2003, **42**, 2203–2205.
28 S. Y. Ho and E. R. T. Tiekink, *CrystEngComm*, 2007, **9**, 368–378; P. Diversi, A. Cuzzola and F. Ghiotto, *Eur. J. Inorg. Chem.*, 2009, 545–553.
29 I. Schröter and J. Strähle, *Chem. Ber.*, 1991, **124**, 2161–2164; S. S.-Y. Chui, R. Chen and C.-M. Che, *Angew. Chem., Int. Ed.*, 2006, **45**, 1621–1624; S.-Y. Yu, Q.-F. Sun, T. K.-M. Lee, E. C.-C. Cheng, Y.-Z. Li and V. W.-W. Yam, *Angew. Chem., Int. Ed.*, 2008, **47**, 4551–4554; R. J. Puddephatt, *Chem. Soc. Rev.*, 2008, **37**, 2012–2027; O. Crespo, in *Modern Supramolecular Gold Chemistry*, ed. A. Laguna, Wiley-VCH, Weinheim, 2008, pp. 65–131.
30 F. Balzano, A. Cuzzola, P. Diversi, F. Ghiotto and G. Uccello-Barretta, *Eur. J. Inorg. Chem.*, 2007, 5556–5562.
31 W. B. Jones, J. Yuan, R. Narayanaswamy, M. A. Young, R. C. Elder, A. E. Bruce and M. R. M. Bruce, *Inorg. Chem.*, 1995, **34**, 1996–2001.
32 I. O. Koshevoy, L. Koskinen, M. Haukka, S. P. Tunik, P. Y. Serdobintsev, A. S. Melnikov and T. A. Pakkanen, *Angew. Chem., Int. Ed.*, 2008, **47**, 3942–3945.

33 I. O. Koshevoy, A. J. Karttunen, S. P. Tunik, M. Haukka, S. I. Selivanov, A. S. Melnikov, P. Y. Serdobintsev, M. A. Khodorkovskiy and T. A. Pakkanen, *Inorg. Chem.*, 2008, **47**, 9478–9488.
34 R. Uson, A. Laguna and M. Laguna, *Inorg. Synth.*, 1989, **26**, 85–91.
35 M. T. Raisanen, N. Runeberg, M. Klinga, M. Nieger, M. Bolte, P. Pyykko, M. Leskela and T. Repo, *Inorg. Chem.*, 2007, **46**, 9954–9960.
36 R. A. Baldwin and M. T. Cheng, *J. Org. Chem.*, 1967, **32**, 1572–1577.
37 I. O. Koshevoy, Y.-C. Lin, A. J. Karttunen, M. Haukka, P.-T. Chou, S. P. Tunik and T. A. Pakkanen, *Chem. Commun.*, 2009, 2860–2862.
38 *DATAMAX, 2.20*, Jobin Yvon, Inc., Edison, N. J., 2001.
39 *Origin, 5.0*, Microcal Software, Inc., Northampton, M. A., 1997.
40 Z. Otwinowski and W. Minor, in *Macromolecular Crystallography, part A*, ed. J. Carter, C. W. and R. M. Sweet, Academic Press, New York, 1997, vol. 276, pp. 307–326.
41 A. J. M. Duisenberg, L. M. J. Kroon-Batenburg and A. M. M. Schreurs, *J. Appl. Crystallogr.*, 2003, **36**, 220–229.
42 G. M. Sheldrick, *Acta Crystallogr., Sect. A: Found. Crystallogr.*, 2008, **A64**, 112–122.
43 A. Altomare, M. C. Burla, M. Camalli, G. L. Cascarano, C. Giacovazzo, A. Guagliardi, A. G. G. Moliterni, G. Polidori and R. J. Spagna, *J. Appl. Crystallogr.*, 1999, **32**, 115–119.
44 L. Palatinus and G. Chapuis, *J. Appl. Crystallogr.*, 2007, **40**, 786–790.
45 L. J. Farrugia, *J. Appl. Crystallogr.*, 1999, **32**, 837–838.
46 G. M. Sheldrick, *SADABS-2008/1 - Bruker AXS area detector scaling and absorption correction*, Bruker AXS, Madison, Wisconsin, USA, 2008.
47 R. J. Cooper, R. O. Gould, S. Parsons and D. J. Watkin, *J. Appl. Crystallogr.*, 2002, **35**, 168–174.
48 A. D. Becke, *J. Chem. Phys.*, 1993, **98**, 5648–5652.
49 M. J. Frisch, G. W. Trucks, H. B. Schlegel, G. E. Scuseria, M. A. Robb, J. R. Cheeseman, J. A. Montgomery, Jr., T. Vreven, K. N. Kudin, J. C. Burant, J. M. Millam, S. S. Iyengar, J. Tomasi, V. Barone, B. Mennucci, M. Cossi, G. Scalmani, N. Rega, G. A. Petersson, H. Nakatsuji, M. Hada, M. Ehara, K. Toyota, R. Fukuda, J. Hasegawa, M. Ishida, T. Nakajima, Y. Honda, O. Kitao, H. Nakai, M. Klene, X. Li, J. E. Knox, H. P. Hratchian, J. B. Cross, V. Bakken, C. Adamo, J. Jaramillo, R. Gomperts, R. E. Stratmann, O. Yazyev, A. J. Austin, R. Cammi, C. Pomelli, J. W. Ochterski, P. Y. Ayala, K. Morokuma, G. A. Voth, P. Salvador, J. J. Dannenberg, V. G. Zakrzewski, S. Dapprich, A. D. Daniels, M. C. Strain, O. Farkas, D. K. Malick, A. D. Rabuck, K. Raghavachari, J. B. Foresman, J. V. Ortiz, Q. Cui, A. G. Baboul, S. Clifford, J. Cioslowski, B. B. Stefanov, G. Liu, A. Liashenko, P. Piskorz, I. Komaromi, R. L. Martin, D. J. Fox, T. Keith, M. A. Al-Laham, C. Y. Peng, A. Nanayakkara, M. Challacombe, P. M. W. Gill, B. Johnson, W. Chen, M. W. Wong, C. Gonzalez, J. A. Pople, *Gaussian 03, Revision C.02*, Gaussian, Inc., Wallingford CT, 2004.
50 R. G. Parr and W. Yang, *Density-Functional Theory of Atoms and Molecules*, Oxford University Press, New York, 1989; R. E. Stratmann, G. E. Scuseria, M. J. Frisch, *J. Chem. Phys.*, 1998, 109, 8218-8225.
51 A. Schäfer, C. Huber and R. Ahlrichs, *J. Chem. Phys.*, 1994, **100**, 5829–5835; C. Lee, W. Yang and R. G. Parr, *Phys. Rev. B*, 1988, **37**, 785–789; A. Schäfer, H. Horn and R. Ahlrichs, *J. Chem. Phys.*, 1992, **97**, 2571–2577.
52 D. Andrae, U. Häußermann, M. Dolg, H. Stoll and H. Preuß, *Theor. Chim. Acta*, 1990, **77**, 123–141.
53 A. Battisti, O. Bellina, P. Diversi, S. Losi, F. Marchetti and P. Zanello, *Eur. J. Inorg. Chem.*, 2007, 865–875.
54 K. Nomiya, N. C. Kasuga, I. Takamori and K. Tsuda, *Polyhedron*, 1998, **17**, 3519–3530; R. Noguchi, A. Hara, A. Sugie and K. Nomiya, *Inorg. Chem. Commun.*, 2006, **9**, 60–63.
55 R. Narayanaswamy, M. A. Young, E. Parkhurst, M. Ouellette, M. E. Kerr, D. M. Ho, R. C. Elder, A. E. Bruce and M. R. M. Bruce, *Inorg. Chem.*, 1993, **32**, 2506–2517.
56 M. Bardaji, M. J. Calhorda, P. J. Costa, P. G. Jones, A. Laguna, M. R. Perez and M. D. Villacampa, *Inorg. Chem.*, 2006, **45**, 1059–1068.
57 W. J. Hunks, M. C. Jennings and R. J. Puddephatt, *Inorg. Chem.*, 2000, **39**, 2699–2702.
58 J. Vicente and M. T. Chicote, *Coord. Chem. Rev.*, 1999, **193–195**, 1143–1161.
59 O. Crespo, F. Canales, M. C. Gimeno, P. G. Jones and A. Laguna, *Organometallics*, 1999, **18**, 3142–3148.
60 P. Pyykko, *Angew. Chem., Int. Ed.*, 2004, **43**, 4412–4456.
61 H. Schmidbaur and A. Schier, *Chem. Soc. Rev.*, 2008, **37**, 1931–1951.
62 A. Sladek and H. Schmidbaur, *Chem. Ber.*, 1995, **128**, 907–909; J. M. López-de-Luzuriaga, A. Sladek, W. Schneider and H. Schmidbaur, *Chem. Ber.*, 1997, **130**, 641–646; S. Wang and J. P. J. Fackler, *Inorg. Chem.*, 1990, **29**, 4404–4407; E. Barreiro, J. S. Casas, M. D. Couce, A. Gato, A. Sanchez, J. Sordo, J. M. Varela and E. M. Vazquez Lopez, *Inorg. Chem.*, 2008, **47**, 6262–6272.
63 A. Sladek and H. Schmidbaur, *Inorg. Chem.*, 1996, **35**, 3268–3272.
64 V. W.-W. Yam, S. W.-K. Choi and K.-K. Cheung, *Organometallics*, 1996, **15**, 1734–1739.
65 M. A. Rawashdeh-Omary, M. A. Omary and H. H. Patterson, *J. Am. Chem. Soc.*, 2000, **122**, 10371–10380.
66 P. Fischer, A. Ludi, H. H. Patterson and A. W. Hewat, *Inorg. Chem.*, 1994, **33**, 62–66; Z. Assefa, B. G. McBurnett, R. J. Staples and J. P. Fackler, *Inorg. Chem.*, 1995, **34**, 4965–4972; A. Burini, R. Bravi, J. P. J. Fackler, R. Galassi, T. A. Grant, M. A. Omary, B. R. Pietroni and R. J. Staples, *Inorg. Chem.*, 2000, **39**, 3158–3165.
67 Y.-A. Lee, J. E. McGarrah, R. J. Lachicotte and R. Eisenberg, *J. Am. Chem. Soc.*, 2002, **124**, 10662–10663; B. Weissbart, D. V. Toronto, A. L. Balch and D. S. Tinti, *Inorg. Chem.*, 1996, **35**, 2490–2496.
68 U. Helmstedt, S. Lebedkin, T. Hocher, S. Blaurock and E. Hey-Hawkins, *Inorg. Chem.*, 2008, **47**, 5815–5820.
69 F. Jensen, *Introduction to Computational Chemistry*, 2 edn, John Wiley & Sons, Chichester, 2006.
70 S. J. A. van Gisbergen, J. A. Groeneveld, A. Rosa, J. G. Snijders and E. J. Baerends, *J. Phys. Chem. A*, 1999, **103**, 6835–6844; E. J. Fernandez, M. C. Gimeno, A. Laguna, J. M. Lopez-de-Luzuriaga, M. Monge, P. Pyykko and D. Sundholm, *J. Am. Chem. Soc.*, 2000, **122**, 7287–7293; P. Pyykkö, *Chem. Soc. Rev.*, 2008, **37**, 1967–1997.

